

Field Survey of the Samoa Tsunami of 29 September 2009

Emile A. Okal,¹ Hermann M. Fritz,² Costas E. Synolakis,^{3,4} José C. Borrero,^{3,5} Robert Weiss,⁶ Patrick J. Lynett,⁷ Vasily V. Titov,⁸ Spyros Foteinis,⁴ Bruce E. Jaffe,⁹ Philip L.-F. Liu,¹⁰ and I-chi Chan¹⁰

Online material: Full dataset of surveyed amplitudes.

INTRODUCTION

On 29 September 2009, a strong earthquake took place south of the Samoa Islands in the southcentral Pacific. It triggered a local tsunami, which caused considerable damage and 189 fatalities on the Samoa Islands and in the northern Tonga archipelago. We present here the results of a tsunami survey conducted by an International Tsunami Survey Team in the Samoa Islands on 4–10 October 2009 and in northern Tonga on 25–27 November 2009.

The Earthquake of 29 September 2009: Geographical Background

The earthquake occurred at 17:48:10 GMT (local time 06:48 on the 29th in Samoa; on the 30th in Tonga), with a source located at 15.51°S and 172.03°W and a focal depth estimated at 18 km by the U.S. Geological Survey (USGS). The epicenter is thus 200 km south of the Samoa Islands and 350 km NNE of the principal groups of Tonga (Figure 1). Note however, the presence of a small island, Niuaotupapu, only 200 km WSW of the epicenter.

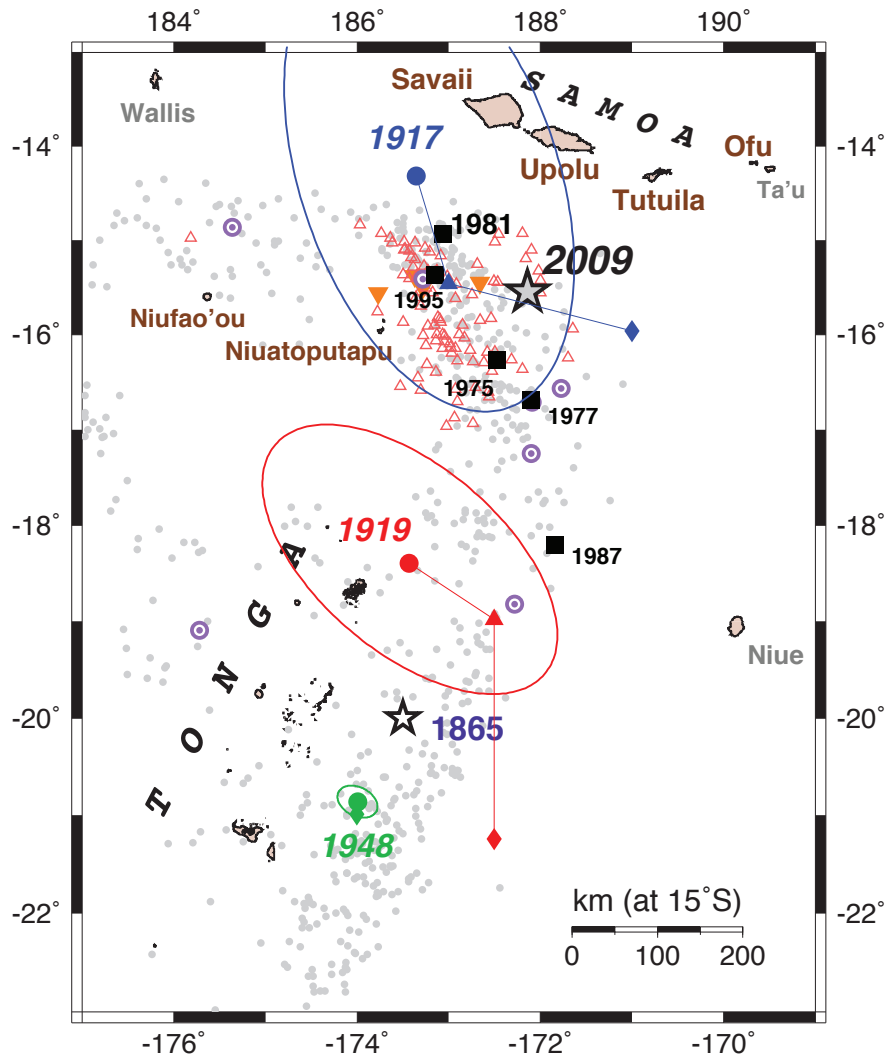
The Samoa Islands comprise the territory of American Samoa, which regroups the island of Tutuila (142 km²; capital: Pago Pago), and the islets of Ofu, Olosega, Ta'u, Rose, and Swains, and the independent country of Samoa (formerly Western Samoa), comprised of the islands of Upolu (1,125 km²; capital: Apia), Savai'i (1,708 km²), and a few islets including Manono. The island of Niuaotupapu, the nearby islet of Tafahi, and the more distant island of Niuafo'ou belong to the Kingdom of Tonga.

Plate Tectonics Background

The Samoa Islands are located 200 km north of the bend in the boundary of the Pacific plate marking the termination of the Kermadec-Tonga subduction zone. The convergent boundary expressing the subduction of the Pacific plate under the Australian one gives way to a strike-slip regime along a transform fault running north of the Fiji Islands, and linked across a spreading center in the Fiji Basin to a similar system in the Loyalty Islands, eventually connecting to the Vanuatu subduction zone. During the transition from the Tonga subduction to the Fiji transform, the Pacific plate undergoes a lateral tear described by Govers and Wortel (2005) as a “Subduction Transform Edge Propagator” (STEP). Relevant seismicity features normal faulting and has been documented in comparable environments, notably in the Loyalty Islands and in the South Sandwich Islands (Okal and Hartnady 2009).

The Samoa Islands constitute a complex volcanic system, since the youngest, historically active, least eroded, and hence largest, island is the westernmost one, Savai'i. This would contradict the classical hotspot paradigm (Natland 1980), which is generally followed by most other island chains in the Pacific. The recent identification of activity at Vailulu'u Seamount, at the east end of the chain (Hart *et al.* 2000), and the dating of the early phases of shield-building of Savai'i to 5 Ma can be reconciled with the motion of the Pacific plate over a fixed hotspot (Koppers *et al.* 2008). The island of Savai'i simply continues to be active through a poorly understood mechanism, whereas Upolu and Tutuila have been inactive for about 1 m.y. (Workman *et al.* 2004). Because of its proximity to the plate boundary, the Samoa volcanic unit could affect the local seis-

1. Department of Earth and Planetary Sciences, Northwestern University, Evanston, IL 60208
2. School of Civil and Environmental Engineering, Georgia Institute of Technology, Savannah, GA 31407
3. Department of Civil Engineering, University of Southern California, Los Angeles, CA 90089
4. Department of Environmental Engineering, Technical University of Crete, 73100 Chania, Greece
5. ASR Ltd., 1 Wainui Road, Raglan 3225, New Zealand
6. Department of Geology & Geophysics, Texas A&M University, College Station, TX 77843
7. Zachry Department of Civil Engineering, Texas A&M University, College Station, TX 77843
8. Pacific Marine Environmental Laboratories, NOAA, 7600 Sand Point Way NE, Seattle, WA 98115
9. USGS Pacific Science Center, 400 Natural Bridges Drive, Santa Cruz, CA 95060
10. School of Civil and Environmental Engineering, Cornell University, Ithaca, NY 14853



▲ Figure 1. Location map of the 2009 Samoa epicenter (large gray star) and related events. The boundary of the Pacific plate is defined by the database of CMT solutions shallower than 50 km (small gray dots); those with a moment greater than 10^{26} dyn*cm are shown as bull's eye symbols. The great earthquakes of 26 June 1917, 30 April 1919, and 08 September 1948 were relocated using the algorithm of Wyession *et al.* (1991); for each of them, the solid dot represents our relocation (with confidence ellipse), the triangle Gutenberg and Richter's (1954) epicenter, and the diamond the ISS solution. The black squares show earthquakes located north of 18° S for which there exists a confirmed record of a tsunami; the inverted triangles are relocated epicenters of other events predating 1963 with at least one magnitude > 7 and without tsunami reports. The small red open triangles are earthquakes occurring during a 24-hr window following the mainshock of 29 September 2009. Note that they are significantly shifted from the latter's location, and are therefore not conventional aftershocks. Adapted from Okal *et al.* (2004).

mic regime, and in particular the STEP system, in a way that remains, however, subject to speculation.

Niuatoputapu (18 km²; pop. 930; max. altitude 157 m a.s.l.) is a coral-reefed volcanic island dated to 3 Ma, while its neighbor Tafahi (3.4 km²; pop. 100; max. altitude 560 m a.s.l.) is a smaller and steeper volcanic cone that probably last erupted in the Holocene. The volcanism at both islands expresses a complex mixture of classical back-arc volcanism, and interaction with the Samoan plume and with subducted remnants of the Louisville plume (Wendt *et al.* 1997; Turner and Hawkesworth 1997). To the west, the volcanism of Niuafu'ou (15 km²; pop. 700; max. elev. 260 m a.s.l.) may be more directly related to spreading in the Lau Basin (Turner

and Hawkesworth 1997); its last eruption dates back to 1985 (Regelous *et al.* 2008).

Fundamental Seismological Data

Immediate assessments of the seismic moment of the Samoa earthquake were given as 1.2×10^{28} dyn*cm (USGS); 1.82×10^{28} dyn*cm (Global Centroid Moment Tensor [CMT] project); and 1.7×10^{28} dyn*cm (Centre Polynésien de Prévention des Tsunamis [Tahiti]). Later and more elaborate solutions include Li *et al.*'s (2009) composite mechanism (with a total moment of 1.8×10^{28} dyn*cm), and Lay *et al.*'s (2009) *W*-phase inversion (2.1×10^{28} dyn*cm). We will retain a value of 1.8×10^{28} dyn*cm, corresponding to a "moment magnitude" $M_w = 8.1$.

All moment tensor inversions available to date yield a normal faulting mechanism, with generally one fault plane trending north–south, but whose azimuth varies from 345° to $7(367)^\circ$. The choice of the fault plane is made difficult by the fact that the numerous events subsequent to the mainshock cluster away from it (Figure 1), and also feature a diversity of focal mechanisms differing strongly from that of the mainshock. As such, these later events are not traditional aftershocks occurring on the fault plane, but rather represent seismicity probably triggered by regional stress transfer outside the fault area of the mainshock. This pattern is indeed reminiscent of the seismicity following the great normal faulting Sanriku, Japan earthquake of 02 March 1933 (Kirby *et al.* 2008).

Another singular aspect of the 2009 Samoa earthquake is that the non-double-couple component of its CMT solution is particularly strong, with the characteristic parameter ϵ reaching 0.15 to 0.30 in the various inversions, while it rarely exceeds a few percent for most subduction zone earthquakes. This could indicate a complex source process, involving for example a bifurcation of the rupture during faulting, or the combination of an outer rise mainshock and a triggered rupture on the interplate contact, as suggested by Li *et al.* (2009).

The slowness parameter θ , introduced by Newman and Okal (1998), takes the value -4.82 , which characterizes the event as moderately fast, *i.e.*, producing accelerations slightly stronger than would be expected from its seismic moment under conventional seismic scaling laws. Again, this pattern is in general agreement with the intraplate character of the event.

Predecessors

The 2009 Samoa earthquake has no comparable predecessor in the era of modern seismic instrumentation, *i.e.*, in the past 50 years. The strongest earthquake during that period is that of 01 September 1981, whose moment is 10 times smaller (1.9×10^{27} dyn*cm), and which generated a relatively weak tsunami, causing some flooding on Savai'i, but neither structural damage nor casualties (Solov'ev *et al.* 1986). Its mechanism represents a tear in the Pacific plate, along the geometry predicted by the STEP paradigm (Govers and Wortel 2005).

Benign tsunamis were also recorded on maregraphs with at most decimetric amplitudes during the earthquakes of 26 December 1975, 02 April 1977, 06 October 1987, and 07 April 1995. These events are shown as black squares on Figure 1.

However, historical archives mention a violent tsunami on 26 June 1917, following an earthquake which, in this respect, could be regarded as a predecessor to the 2009 event. We relocated this event on the basis of arrival times published by the International Seismological Summary (ISS), using the interactive method of Wyssession *et al.* (1991). The solution converges to 14.37°S , 173.35°W (Okal *et al.* 2004), but given the imprecision of this dataset, the confidence ellipse is very large, and does include the 2009 epicenter (Figure 1). Mantle magnitudes obtained from Wiechert records at Uppsala (Okal 1992) and Galitzin records at De Bilt, suggest a moment $M_0 = 8.5 \times 10^{27}$ dyn*cm, within a multiplicative or divisive factor of 2.5. This range includes the moment of the 2009 shock (1.8×10^{28}

dyn*cm). It is however improbable that the 1917 and 2009 earthquakes would be repeat events involving subsequent ruptures of the same material, since estimates of repeat times for intraplate earthquakes, and in particular outer rise events, are generally considerably longer (S. Kirby, personal communication, 2009), and we prefer to consider the 1917 and 2009 shocks as similar earthquakes occurring on neighboring but distinct segments of the outer-rise–STEP system.

The earthquake of 26 June 1917 generated a tsunami which, according to Solov'ev and Go (1984), ran up to 12 m in Samoa, although the exact location of this report is not given. This tsunami was confirmed by two witnesses interviewed during a later survey, independently of our team (C. Chagué-Goff, personal communication, 2009), who reported that their grandmother had run away from the wave in Apia in 1917. On the other hand, during our field surveys, we were unable to identify any other witnesses whose ancestors would have kept and transmitted memories of what should have been a catastrophic human disaster. The situation is made more complex by the fact that some catalogs also mention a tsunami on 01 May 1917, *i.e.*, 57 days earlier, with the same run-up of 12 m in Samoa. The earthquake of 01 May 1917 is well located, in the Kermadec Islands, more than 1,700 km farther south, and does not appear to be systematically larger than that of 26 June (Okal 1992); this led Solov'ev and Go (1984) to question the figure of 12 m on 01 May 1917, which could simply be attributed to an error in the date of the report.

Other historical earthquakes with at least one published magnitude greater than 7, but no reported tsunami, are known in the area on 08 January 1939, 29 June 1948 (probably at intermediate depth), 18 April 1949, and 14 April 1957. Their relocated epicenters are shown as solid inverted triangles on Figure 1 (the 1949 and 1957 events plot essentially at the same location as the 1995 epicenter).

Farther south, the earthquake of 17 November 1865 generated a transoceanic tsunami (Okal *et al.* 2004), also described qualitatively in Tonga, and the great earthquake of 30 April 1919 generated a tsunami that locally ran up to 2.5 m in Tonga, but was not reported in Samoa. A tsunami was recorded in Samoa with an amplitude of 10 cm from the Tongan earthquake of 08 September 1948, although no direct reports are available in the epicentral area (Solov'ev and Go 1984).

The Tsunami of 29 September 2009

The earthquake of 29 September 2009 generated a tsunami that reached the Samoa Islands in about 15 to 20 minutes, and caused particularly intense destruction on the southeastern coast of Upolu, but largely spared the northern shore, where the capital city of independent Samoa, Apia, is located. By contrast, on the island of Tutuila (American Samoa), considerable damage was wrought both on the southern and northern coasts, although the latter being of more difficult access, is much less populated. The present, and probably definitive, human death toll is 34 on American Samoa, 146 in (independent) Samoa, and 9 on the Tongan island of Niuaotupapu, for a total of 189 persons killed. Economic losses are estimated conservatively at US\$200 million.

These figures make the 2009 Samoa tsunami the deadliest documented tsunami in the region (allowing for the very vague information on the 1917 tsunami), or even in the entire portion of the South Pacific extending from New Britain (where the 1937 explosion of Rabaul caldera killed 500 people, including some from the tsunami), all the way to, and excluding, the South American coast. The 2009 tsunami is also the first one since 1964 that resulted in human life loss on U.S. soil (if we exclude the Kalapana, Hawaii, tsunami of 29 November 1975, which drowned two hikers camping on Halape Beach, but caused no damage to infrastructure).

The Pacific Tsunami Warning Center (PTWC) located in Ewa Beach, Hawaii, issued an alert 16 minutes after the origin time of the earthquake (Hirshorn *et al.* 2009), a delay typical of its operations and adequate for the purpose of distant warning, but which precluded its use in the near field, since the first waves reached the Samoa Islands within 15 to 20 minutes after origin time. This reinforces the concept that real-time tsunami mitigation in the near field must rely on self-evacuation, to be triggered by the affected populations themselves, upon feeling the earthquake or observing any anomalous behavior in the level of the sea. Such warning must be individual, or organized at the strictly local level of a village or small town, and cannot depend on a centralized warning entity.

TSUNAMI SURVEY IN THE SAMOA ISLANDS

General Logistics

In the hours following the tsunami, an International Tsunami Survey Team was assembled, comprising the authors of the paper, along the lines of similar surveys carried out following all major tsunamis in the past 17 years (Synolakis and Okal 2005); most members of this group were able to reach Pago Pago in the evening of Sunday, 04 October, and to start surveying in the field Monday morning 05 October, exactly six days after the tsunami. This delay is optimal in that it allows prior completion of search and rescue operations, while remaining short enough to prevent both clean-up efforts and any heavy meteorological storm from having eradicated critical watermarks or any other inundation evidence, which are by nature fragile and ephemeral. Additional surveying was performed by independent teams, notably on American Samoa (*e.g.*, Koshimura *et al.* 2009; Jaffe *et al.* 2009), and on the French territory of Wallis and Futuna to the west (Lamarche *et al.*, 2010).

Given the number of participants, and the size of the islands to be covered, the team generally operated in subgroups of two to three investigators. The islands of Tutuila and Ofu in American Samoa were covered from 05 to 07 October, with several locations on the northern shore of Tutuila surveyed by boat on 08–10 October. Upolu, Savai'i, and Manono in independent Samoa were surveyed from 08 to 10 October. The team left the field on Saturday, 11 October 2009, after complementary work on Tutuila.

In the immediate aftermath of the tsunami, commercial air service to Niuatoputapu was interrupted due to littering of the grass runway by tsunami debris, and thus the survey on that

remote Tongan island was delayed until late November. The island, and its neighbor Tafahi, were visited by Fritz and Okal on 25–27 November 2009. On the way back, a short stopover was made at the island of Niuafu'ou, 200 km to the west.

Methodology

The survey used conventional methods consisting of measuring the penetration of the waves and organizing it into a homogeneous scientific database. We define *Inundation* as the maximum horizontal extent of penetration of the waves; *Flow Depth* as the thickness of the water column that passed through a reference point (most often the shoreline), and *Run-up* as the altitude above sea level (corrected for tides) of the point of extreme penetration, where inundation is measured.

Run-up often represents the most definitive parameter, as it gives the minimum altitude defining the safety zone that the tsunami did not reach. However, in the case of extended shallow coastal plains, run-up can occasionally be less than flow depth at the shore, and in such cases, flow depth becomes a better estimate of the vertical extent of the tsunami.

The penetration of the wave is identified both from *evidence* deposited by the waves, either physical (in the form of all sorts of debris, sedimentary deposits, watermarks left on structures, etc.), or chemical (the wave's saltwater leading to rapid death of vegetal species and their discoloration); and from *testimony* of witnesses present during the onslaught of the tsunami. In addition to the geometrical parameters described above, we interview witnesses to collect data on the kinematics of the waves (number, relative size, temporal separation, polarity of the first wave). Measurements of run-up, flow depth, and inundation are taken using laser ranging and conventional leveling instruments.

As a whole, we obtained 375 tsunami run-up and flow-depth data points in the Samoa Islands and 69 in Tonga. The full dataset is given in the electronic supplement. Figures 2A–H give three-dimensional sketches of our run-up database; when available, we give separate diagrams for flow depths. To enhance legibility, separate plots are shown for the northern and southern shores of Tutuila, and a close-up is given of the bay of Pago Pago.

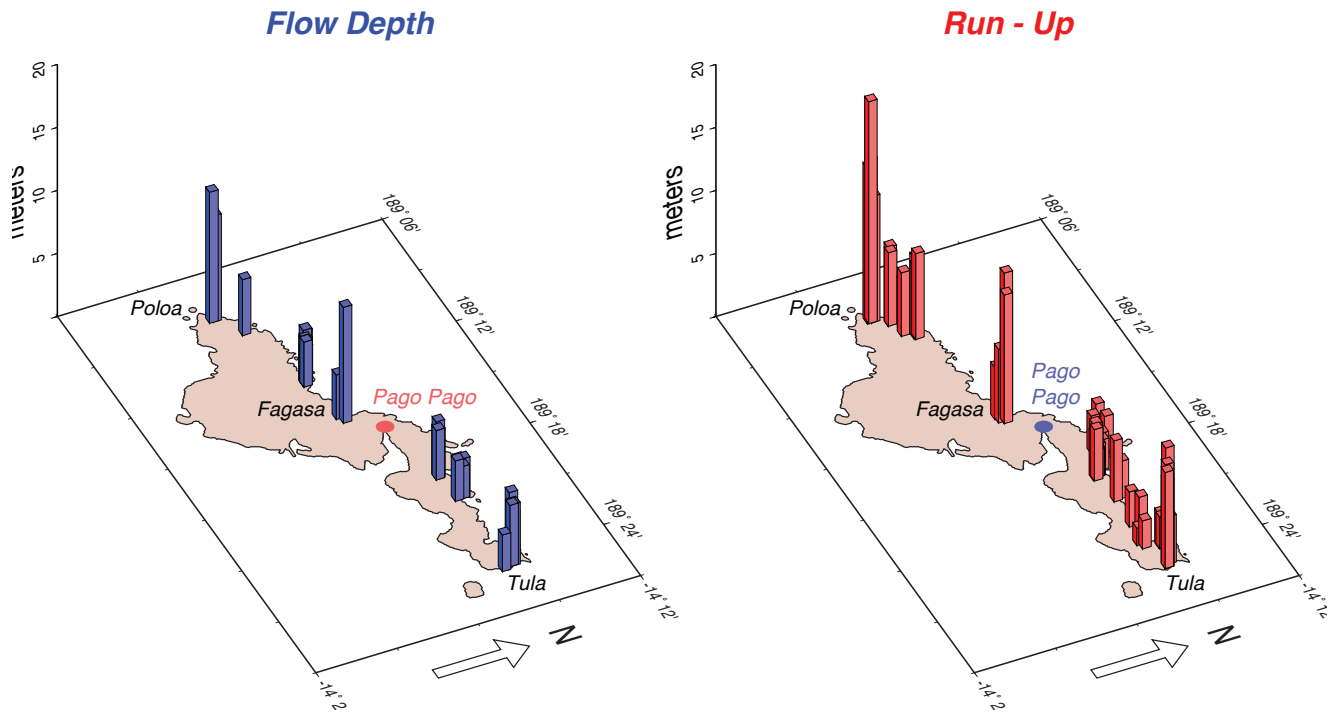
RESULTS

American Samoa

On the island of Tutuila, maximum run-up amplitudes reached 17.6 m in the village of Poloa, located at the western end of the island. In general, the wave amplitude decreases eastward, but remains very large at the eastern end of the island (7.6 m in Tula). In the bays of the north shore, we also surveyed considerable amplitudes (11.9 m in Fagasa).

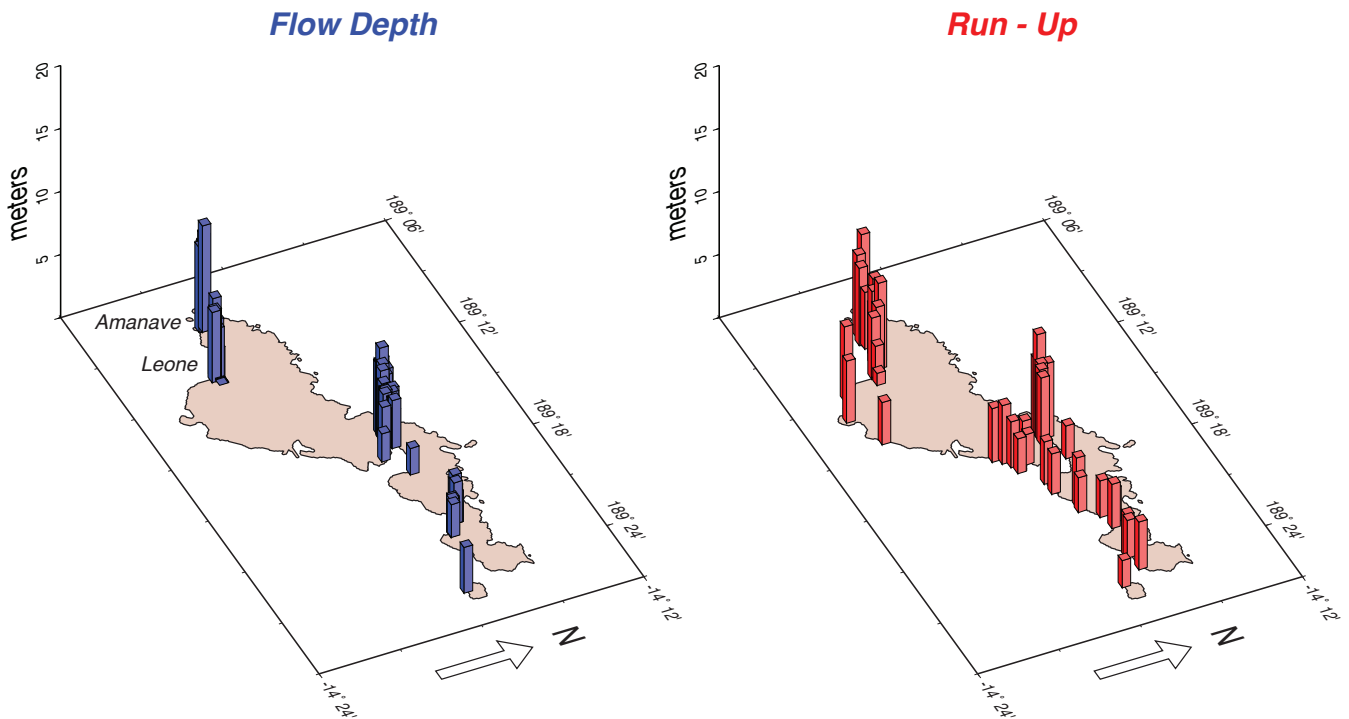
The most substantial damage was wrought in the village of Poloa, where waves destroyed all structures except the church, which was itself severely damaged (Figure 3), and in the city of Leone (the second largest in the territory), where the waterfront was essentially leveled by the tsunami, and inundation reached an impressive 500 m along the bed of the Leafu River.

TUTUILA, AMERICAN SAMOA (North Shore)



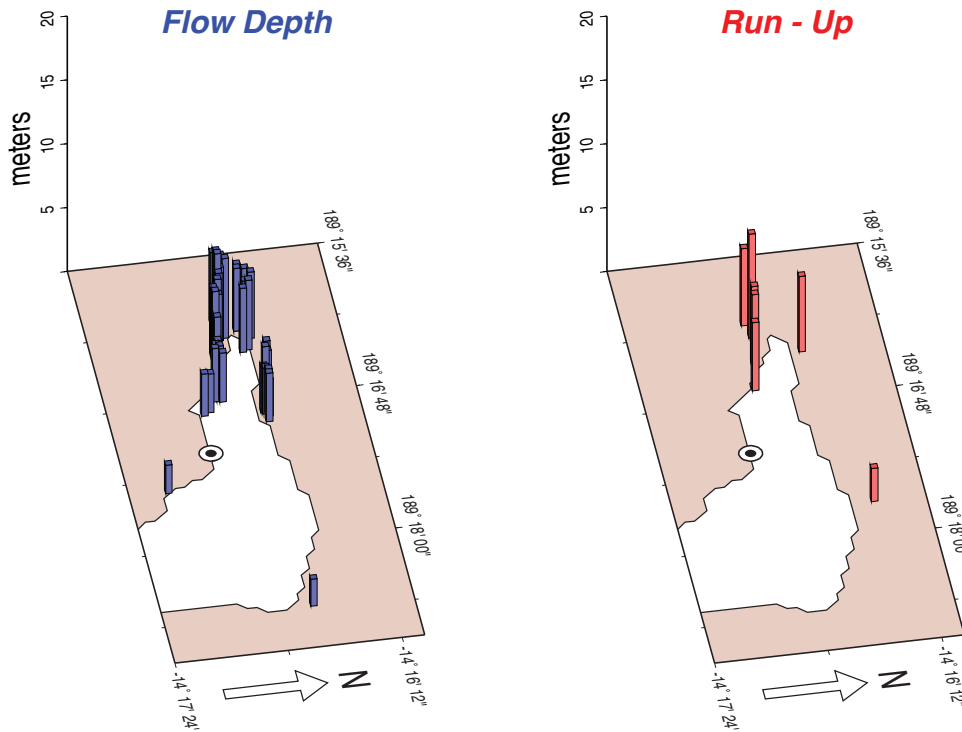
▲ **Figure 2A.** Dataset of flow depth (*left*) and run-up (*right*) heights surveyed on the northern coast of Tutuila.

TUTUILA, AMERICAN SAMOA (South Shore)



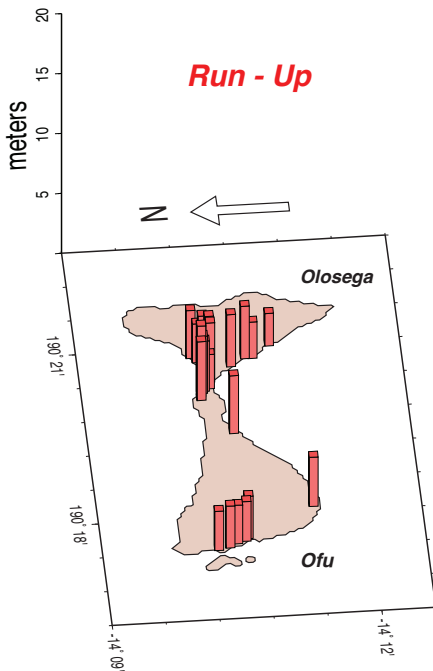
▲ **Figure 2B.** Dataset of flow depth (*left*) and run-up (*right*) heights surveyed on the southern coast of Tutuila.

Close-Up, PAGO PAGO Harbor, American Samoa



▲ **Figure 2C.** Close-up of Figure 2B for PAGO PAGO harbor. The bull's eye symbols show the location of the maregraph that recorded a 2.4-m zero-to-peak wave height (see Figure 7).

OFU and OLOSEGA



▲ **Figure 2D.** Dataset of run-up heights surveyed on Ofu and Olosega.

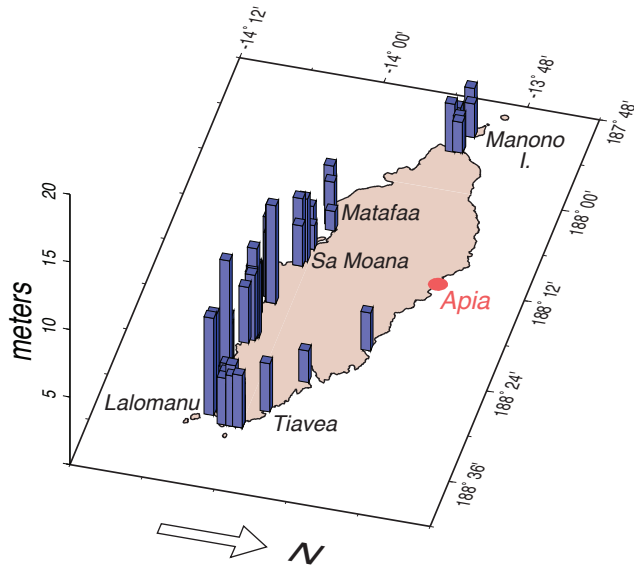
In addition, the capital city of the territory, PAGO PAGO, constitutes a special case, as it is located at the toe of a narrow 4-km-long bay. Surveys showed that the tsunami, which reached at most 3 m at the entrance of the bay, was considerably amplified inside the bay, reaching a run-up of 8 m over an inundation of 538 m at its toe, where it caused considerable damage (destroyed infrastructures, boats and shipping containers carried inland into commercial areas, etc.). While the location of the port in the back of the bay protects it efficiently from certain kinds of short-period storm waves, it unfortunately makes it a “tsunami trap.” The only positive aspect of this geometry is that the largest ocean-going ships usually drop anchor at the entrance of the bay, where the tsunami remained modest, which prevented them from becoming giant projectiles, which could have significantly worsened the damage. Run-up on Ofu was found to be in the 4 m range, with a maximum value of 6 m (Figure 2D).

Given the considerable run-up values, and the scenes of devastation that we witnessed, it is remarkable that only 34 people lost their lives on the island. All the testimonies gathered from survivors reveal a population *educated* about tsunami danger, who self-evacuated upon feeling the earthquake (whose tremors were strong and prolonged, lasting up to 50 s), or upon noticing anomalous activity of the sea.

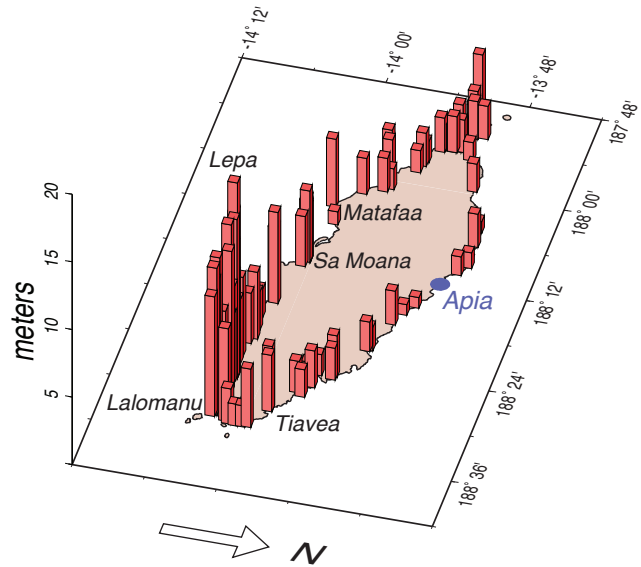
It is possible to analyze the reasons of this generally successful evacuation, which are diverse and may not repeat themselves during the next tsunami. First, one must com-

UPOLU, SAMOA

Flow Depth



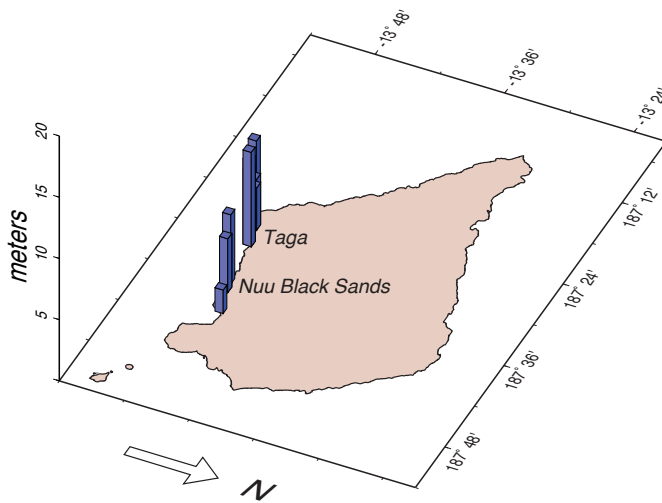
Run - Up



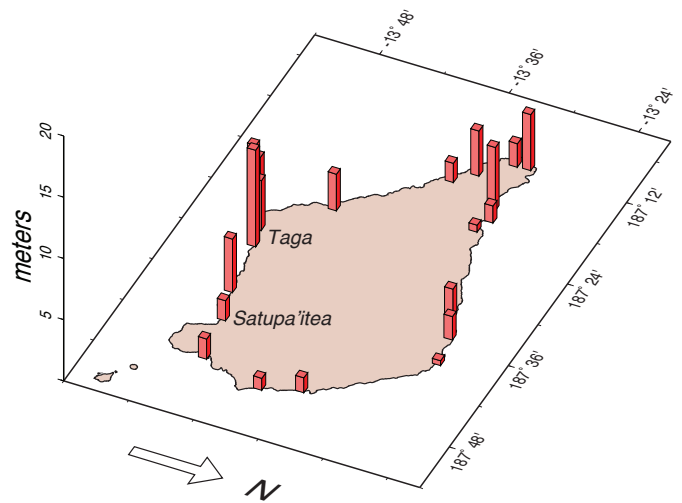
▲ **Figure 2E.** Dataset of flow depth (*left*) and run-up (*right*) heights surveyed on Upolu.

SAVAII, SAMOA

Flow Depth

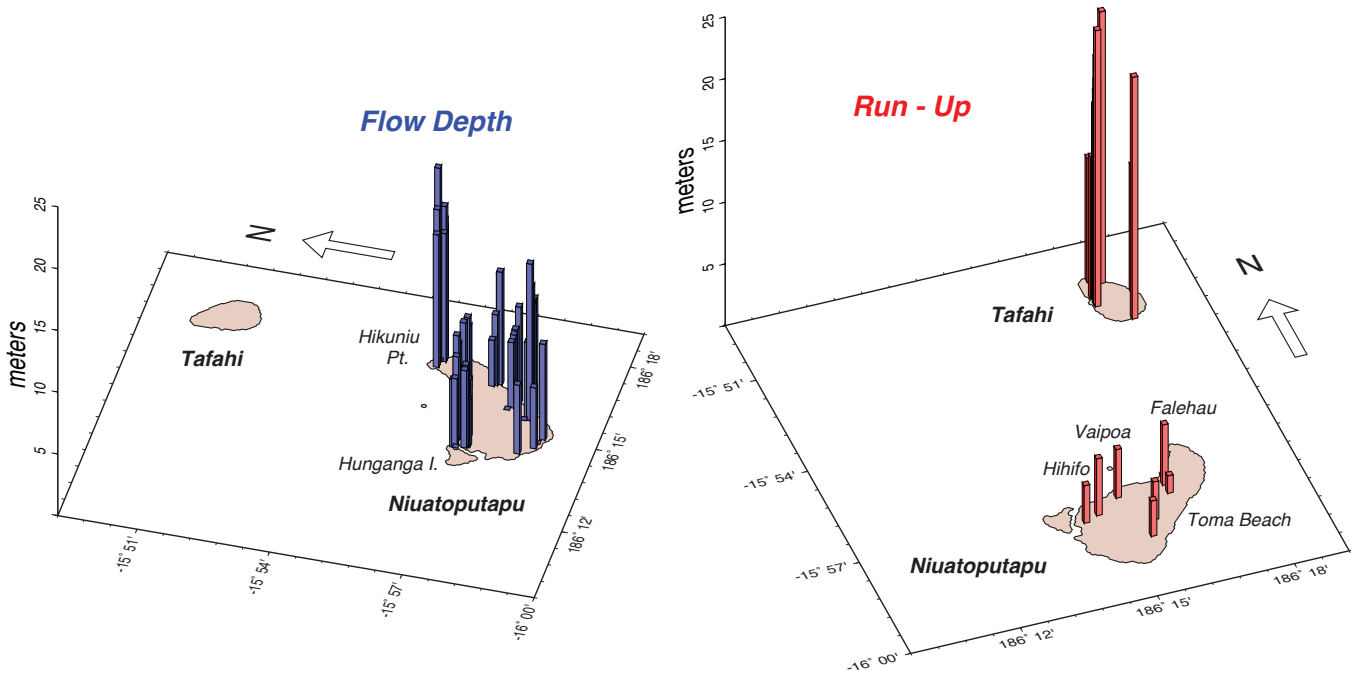


Run - Up



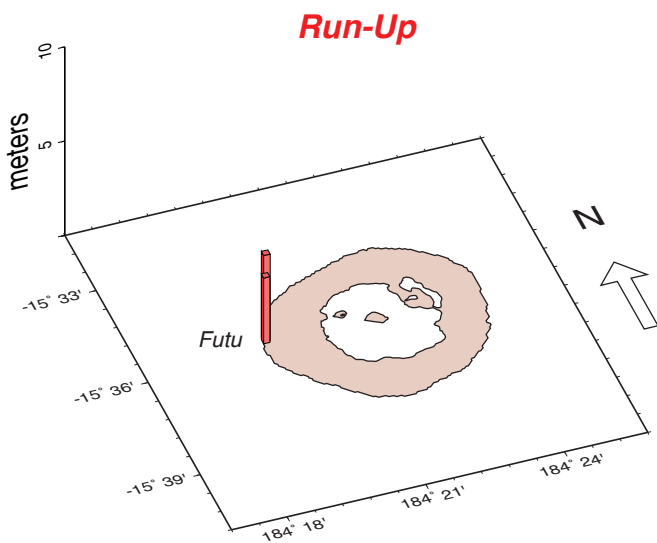
▲ **Figure 2F.** Dataset of flow depth (*left*) and run-up (*right*) heights surveyed on Savai'i.

NORTHERN TONGA



▲ **Figure 2G.** Dataset of flow depth (*left*) and run-up (*right*) heights surveyed on the northern Tongan islands of Niuatoputapu and Tafahi.

NIUAFO'OU



▲ **Figure 2H.** Dataset of run-up heights surveyed on the island of Niuafu'ou (northwestern Tonga).

mend a community that was ready to evacuate, because it was adequately educated. Even though there does not seem to exist, in the Samoa Islands, a broad ancestral memory of tsunami disasters (and surprisingly so, regarding the 1917 event), the population was aware of tsunami danger. In this respect, one could stress the importance of *signage*. All along the coastal highway, we noticed standard blue bilingual signs describing

tsunami danger and instructing people to evacuate upon feeling an earthquake (Figure 4). It is certain that the presence of these signs, which are seen daily by the populations at risk, can eventually instill in them the reflex of self-evacuation. We note however that the signs did not specify *where* to evacuate to.

In addition, a rudimentary but efficient warning system was used by leaders of the villages. We met with elected officials (several mayors, one senator) who described how they used bells and gongs outside their residences to warn their constituents; such systems are used during the more frequent occurrences of cyclones. A very strong community bonding helped save the young, the elderly, and the disabled. We met a resident of Poloa, a village completely destroyed by the tsunami, who evacuated successfully, even though wheelchair-bound. Actually, the only casualty in Poloa was a 68-year-old woman who apparently died from cardiac arrest during the evacuation. The lesson to be learned from these reports is that a successful evacuation does not necessarily require high technology, as long as the local population (including officials in a position of responsibility) is well educated.

There remains the fact that favorable circumstances helped make the evacuation on Tutuila a relative success, and in the first place, the island's topography. The relief of the island is rugged, with steep slopes in the immediate back of many villages, making evacuation out of harm's way easy and fast. In addition, the earthquake occurred at a favorable time, 06:48 AM local time. It was daylight, most people were up and going, having breakfast, children were boarding their school buses, etc. The same tsunami occurring at night and requiring an evacuation under darkness could have been much more lethal.



▲ **Figure 3.** Top: Devastation at Poloa, Tutuila, American Samoa, photographed six days after the event. The church building, behind which the highest run-up on the island, 17.6 m, was measured, is the only building left standing. Bottom: Close-up of a corrugated piece of roofing, wrapped around the pillars of the church porch.

Samoa

In Upolu, the tsunami was particularly devastating along the southeastern shore of the island. Run-up reached 14.5 m at Lepa and 11.4 m at Lalomanu (Figure 2E), where the village was totally destroyed, with 61 casualties. Tsunami amplitudes decrease rapidly westward along the coast, reaching no more than 5 m in Sa Moana and 4.1 m in Matafaa. We note on Figure 2E that the distribution of flow depth along the southern coast of Upolu is more regular. The greater run-up values around Lepa and Lalomanu may express the locally steeper topography of the coastal plain. On the northern coast, we measured 4.8 m at Tiavea in the east, but only 2 to 3 m immediately to the west and no more than 2.5 m along the rest of the northern shore. The tsunami went essentially unnoticed in Apia, where the maregraph registered only 78 cm zero-to-peak.



▲ **Figure 4.** Tsunami Hazard Zone road sign photographed at bus stop in Amanave, Tutuila (American Samoa). Note the pillared construction of the bus stop shelter, providing no cross section for the wave, leaving it undamaged, even though clothing was deposited on its roof, at a height of ~2.5 m. Heavy cast-iron masses (like the one in the back of the shelter) are used as gongs to warn populations of impending disasters (primarily cyclones). Note also the discolored grass on this photograph taken six days after the tsunami.

The situation was similar on the island of Savai'i, where the northern coast was basically spared, while run-up reached 8 m on the southern coast, at Nu'u Black Sands beach, fortunately an uninhabited location. The village of Taga was attacked by a 6-m wave, over a 200-m inundation. Two persons were killed while in the water in Satupa'itea. On Manono, a small (2.5 km²) islet in the Apolima Strait separating Savai'i from Upolu, run-up reached 5.5 m at Apai, and one person was killed.

The death toll of 143 on Upolu is considerably larger than on Tutuila (34 killed), and some discussion of this discrepancy is warranted. The presence of wider coastal plains on Upolu clearly implies a longer evacuation path to the same safe height, meaning that the Upolu shoreline may have been intrinsically more dangerous. To our knowledge, no signage program existed on Upolu, where we saw no signs comparable to that of Figure 4 on Tutuila. On the other hand, evacuation drills had apparently been conducted in a number of communities, even though statements from certain witnesses were contradictory in this respect, and suggested an emphasis on drills along

the northern coast, which was spared by the tsunami. While a meeting of the Pacific Tsunami Warning and Mitigation System had been held in February 2009, there exists no measurement of the effectiveness it may have had in raising the awareness of the local population (D. Mileti, personal communication 2010).

In addition, it appears that a number of victims were swept away inside their vehicles, which they had elected to use in the evacuation, thus contributing to traffic congestion on roads that were often parallel to the coast line. In this respect, the country of Samoa was recovering, at the time of the tsunami, from the “road switch,” an ambitious and intriguing change from keeping right to keeping left on its roads, which had taken place on 07 September 2009, exactly 22 days before the tsunami. Its official motivation referenced global warming and rising sea level, and specifically mentioned evacuation during a tsunami warning. Whatever the political or economic reasons behind the road switch, the arguments given to the inhabitants of Samoa emphasized that their automobiles constituted a line of defense—if not an outright panacea—against threats from the sea, even though well designed tsunami evacuation plans always emphasize the need to evacuate without creating congestion, *i.e.*, by foot or at most on a bicycle.

Niutoputapu, Tonga

This low-lying island at the northern end of the Tonga archipelago suffered a considerable onslaught from the tsunami. Its northern tip, Hikuniu Point, was completely over-run with flow depths on the order of 10 m at elevations of ~6 m. Beaches on the unpopulated southern shores were inundated to distances reaching 950 m at Ve’elolo Beach with flow depths of 10.5 m. At all above locations, the penetration of the tsunami resulted in the total destruction of the existing forests (Figure 5), which thus cannot be envisioned as efficient tsunami barriers under flow depths reaching 10 to 20 m. The airport, located on the southwestern side of the island, was spared, with the grass runway littered with debris, but no damage to the lone airport building where flow depths reached only 20 cm. The three villages on the island are located on the northern side, protected by a 1-km-wide lagoon. The tsunami inflicted significant destruction on many dwellings, with inundation reaching 260 m at Falehau, 143 m at Vaipoa, 585 m in the eastern section of the main village, Hihifo, and 353 m in its western section. Of the nine victims, seven were riding in a pick-up truck swept by the tsunami as it was driving along the main road in Hihifo, parallel to the beach; one was a homeowner who came back to lock his house after initially taking refuge away from the water, and one was the caretaker of the Palm Tree resort on Hunganga, a nearby island separated by a narrow channel, and without any means of evacuation; the otherwise empty resort was totally destroyed.

The pattern of inundation was different on Tafahi, a much steeper stratovolcano protected only by a minimal reef, 8 km northeast of Niutoputapu. Expectedly, inundations distances were shorter, but run-up reached impressive values, typically 10–15 m along most of the island, with a maximum of 22.4 m

measured on the southwestern coast, in the lee of the incoming tsunami, this geometry being reminiscent of the “Babi effect” during the 1992 Flores, Indonesia, tsunami (Yeh *et al.* 1994; Imamura *et al.* 1995; Briggs *et al.* 1995). Fortunately, the only village on Tafahi is built on top of a cliff and accessible only by foot stairs, and it was not reached by the tsunami.

On Niuafu’ou, volcanic cliffs prevail along most of the island, with the villages well sheltered from the sea at an altitude of 50 m. Based on the testimony of inhabitants, we surveyed a run-up of 4.6 m at Futu, the location of the lone wharf (Figure 2H). No damage to the rudimentary infrastructure was observed.

Wave Characteristics

Interviews of several hundred witnesses provide a generally consensual picture of a series of three main waves, the largest one being the third one (or possibly the second one at some sites). Most witnesses on the Samoan Islands described an initial down-draw preceding the first wave, while no consensus was available in this respect in Tonga.

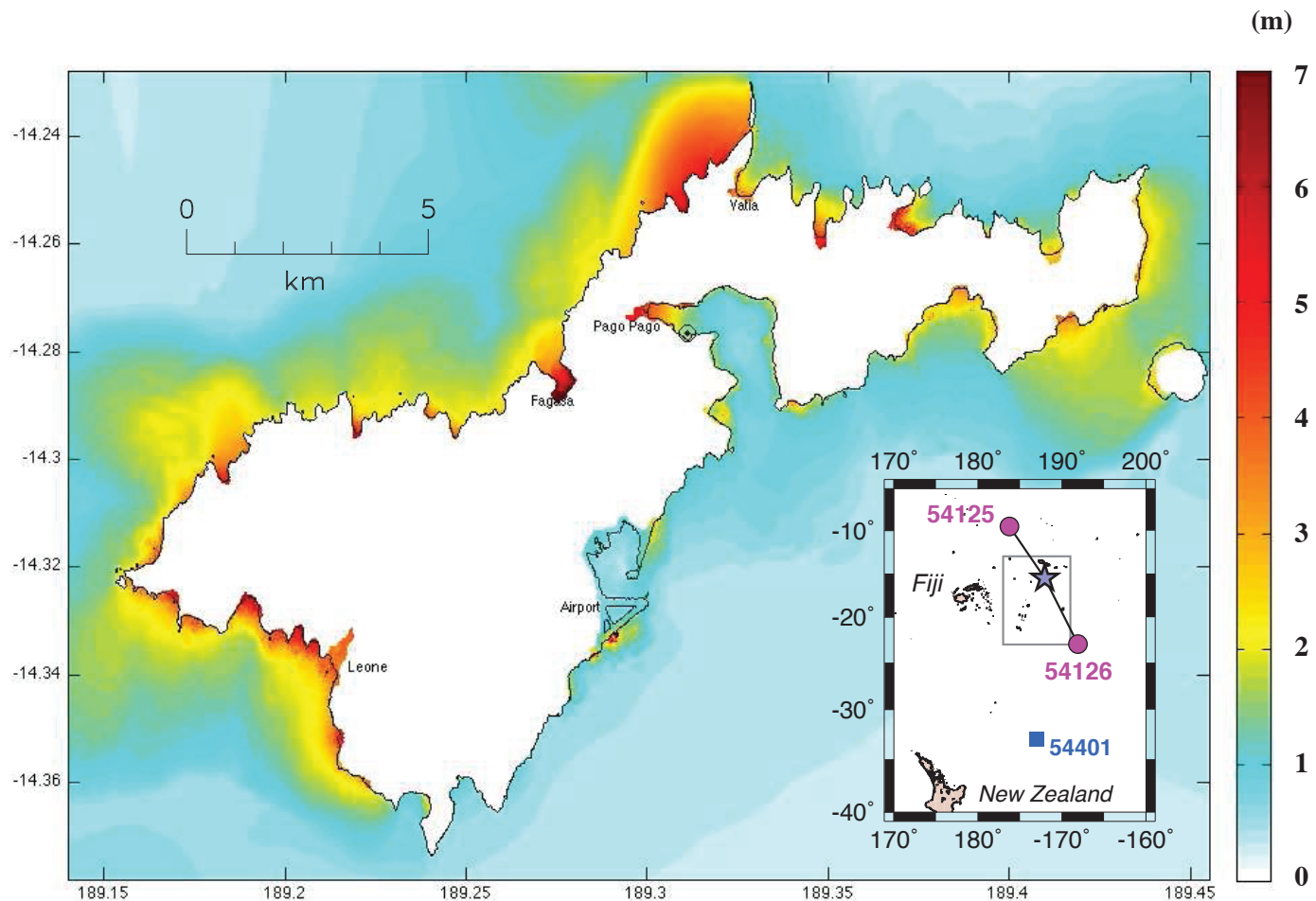
PRELIMINARY MODELING

We present here two preliminary efforts at numerical modeling in the regional field. The first one was carried out at NOAA’s Pacific Marine Environmental Laboratories in quasi real time using the procedure developed by Titov *et al.* (2005), which consists of inverting waveforms from the propagating tsunami as they become recorded by DART sensors, in order to obtain scaling parameters for pre-arranged seismic sources distributed along the plate boundaries of the Pacific Basin. In general, such simulations are not applicable to tsunami warning in the near field, since DART buoys are often located farther from the source than the closest shorelines at risk. For example, in the present case, the closest sensors were DART buoys 51425 (9.49°S; 176.25°W) and 54126 (22.99°S; 168.10°W), which the tsunami reached at 18:51 and 18:53 GMT, respectively 48 and 50 minutes after it hit Upolu and Tutuila. Note that the geometry of the 2009 earthquake is not modeled appropriately by this algorithm, which tacitly assumes a subducting mechanism. Nevertheless, the results of the simulation for Tutuila, shown on Figure 6, correctly predict the extent of inundation in Leone and Pago Pago, and the significant amplitudes of the tsunami in the bays of the north coast (Fagasa, Vatia). This simulation, which required the development of a 30-m grid for the island, was available 48 hours after the event, and was used to prioritize surveying sites on Tutuila.

A number of more detailed and later simulations were performed after our field survey, using the MOST algorithm (Titov and Synolakis 1998), which solves the non-linear equations of hydrodynamics in the shallow-water approximation using the method of alternating steps. First, we modeled the maregram recorded at the entrance of Pago Pago harbor (location shown as a bull’s eye symbol on Figures 2C and 6). This computation is carried out on a three-level telescoping nest of grids, whose resolution ranges from 1.5 arcmin (~2.75 km) in



▲ **Figure 5.** Devastation along Hikuniu Point, at the northeastern corner of Niuaotupapu Island, northern Tonga. The top frame looks west and the bottom one continues it to the right, looking north. The forest was completely taken down by the wave, which reached typical flow depths of 10 m. Note scouring at the base of the tree on the extreme right of the bottom frame. The total span of this view is ~1 km, both frames combined. The island of Tafahi is seen in the distance on the bottom frame.

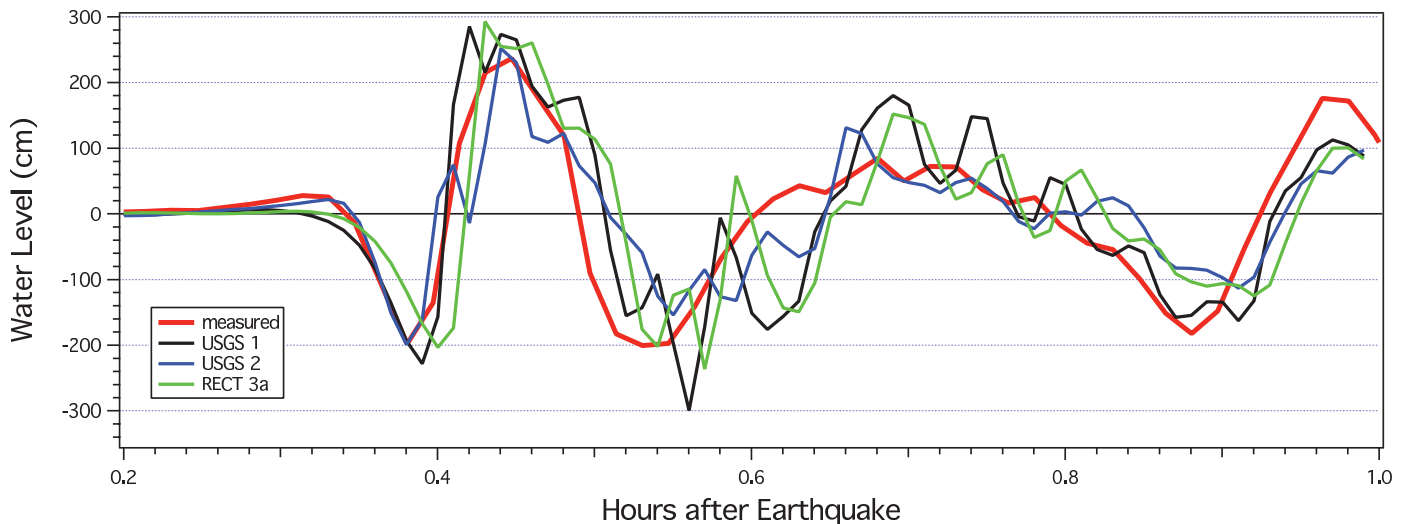


▲ **Figure 6.** Simulation of tsunami inundation for Tutuila, performed in quasi real time using the inversion of records from DART buoys (Titov *et al.* 2005). Note that this model correctly predicts large amplitudes in the bays of the northern coast and substantial inundation in Pago Pago and Leone. The bull's eye symbol shows the location of the maregraph in Pago Pago harbor. The inset shows the location of the two DART buoys used in the inversion (circles), as well as the additional buoy that recorded the tsunami (square). The gray box outlines the boundaries of the map on Figure 1.

the outer grid to 0.5 arcmin (~ 0.9 km) in the intermediate one and finally 0.1 arcmin (~ 180 m) for the innermost grid inside the harbor. The initial wavefield of sea surface deformation, $\eta(x, y; t = 0_+)$, is taken as identical to the static deformation produced at the Earth's surface by the field of seismic slip distributed on the earthquake's fault plane; the latter is computed using Okada's (1985) formalism. This approximation is justified by the fact that even slow seismic sources (which is not the case for the present earthquake) are always hypersonic with respect to typical tsunami phase velocities, even in the shallow water approximation. In Figure 7, we compare the results obtained with three source models. USGS-1 is the slip distribution along the presumed fault plane ($\phi = 343^\circ$; $\delta = 57^\circ$; average rake $\lambda = -61^\circ$; total length ~ 130 km) inverted by the National Earthquake Information Center using the method of Ji *et al.* (2002) and made available 19 hours after the event (G. Hayes, personal communication, 2009). USGS-2 is a hypothetical model where the slip distribution of USGS-1 has been mapped onto the conjugate plane ($\phi = 121^\circ$; $\delta = 46^\circ$; $\lambda = -122^\circ$). While this model has no physical justification, we use it to explore the

robustness of our simulations. Finally, Model RECT-3a considers a rectangular source (110 km \times 50 km) with a uniform slip $\Delta u = 5$ m along the same fault plane as USGS-1. Figure 7 shows that all three models provide an excellent match to the maregram recorded in Pago Pago harbor. In particular, there are no essential differences between the fit of the three models to the recorded maregram. This illustrates the fact that, even at regional distances, and because of its large wavelengths, the tsunami *integrates* the seismic source, with details of its structure becoming largely irrelevant to the final wave heights recorded at the receiver.

Figure 8A shows the simulation on the coarser grid for Model USGS-1. Regarding deep water amplitudes off Tutuila, our results predict strong values at its western tip, as well as comparable amplitudes on the northern and southern shores of the island, in agreement with the results of our survey. By contrast, for Upolu and Savai'i, we predict stronger values on the southern shores than on the northern ones, again in agreement with our field results. Figure 8B shows a close-up of the simulation on Upolu, using the intermediate grid. High deep-water



▲ **Figure 7.** Observed (red) and simulated (other colors) records of the Pago Pago maregraph for the 2009 Samoa tsunami. The three simulations correspond to variations of the seismic source; see text for details. Note the good quality of the fit, which is essentially common to all three models.

amplitudes are indeed predicted at the southeastern tip of the island, where the villages of Lepa and Lalomanu were devastated, but comparable values are expected at the southwestern tip where run-up remained moderate (Figure 2E). This probably illustrates the importance of very fine scale bathymetry in controlling run-up along those various segments of shoreline.

In addition, Figure 8A illustrates the effect of curved shallow bathymetry around the bend of the Tonga arc, in the vicinity of (15.7°S; 173.1°W). This results in strong focusing of the tsunami toward the northern Tonga islands of Niuaotupapu and Tafahi, thus explaining the exceptional run-up and wave heights surveyed on those islands.

CONCLUSION

In conclusion, the 2009 Samoa tsunami constitutes the strongest such event in the region in the past 92 years. The results of our survey constitute a database of close to 400 measurements, with maximum run-up reaching 22.4 m on Tafahi (northern Tonga) and 17.6 m at Poloa (American Samoa), and inundation often extending hundreds of meters inland. These characteristics are well modeled by numerical simulations, even when their source models are rudimentary; in particular, we show that simulations based on the inversion of DART data in quasi real time correctly predicted the main features of inundation around Tutuila, and thus could conceivably be used in the future for search and recovery purposes. The exceptional amplitudes in northern Tonga are explained by focusing due to shallow bathymetry around the Tonga bend. Regarding the societal aspects of the tsunami, and given the surveyed run-up values and the substantial devastation observed, the tsunami could have been much more lethal. On Tutuila (American Samoa), the worst was probably avoided thanks to an educated population that was able to undertake a largely successful self-evacuation. On Upolu, the higher death toll was probably due

to a combination of a greater natural vulnerability of the sites (implying longer evacuation distances), and a less successful response to the process of evacuation, illustrated for example by the absence of systematic signage.

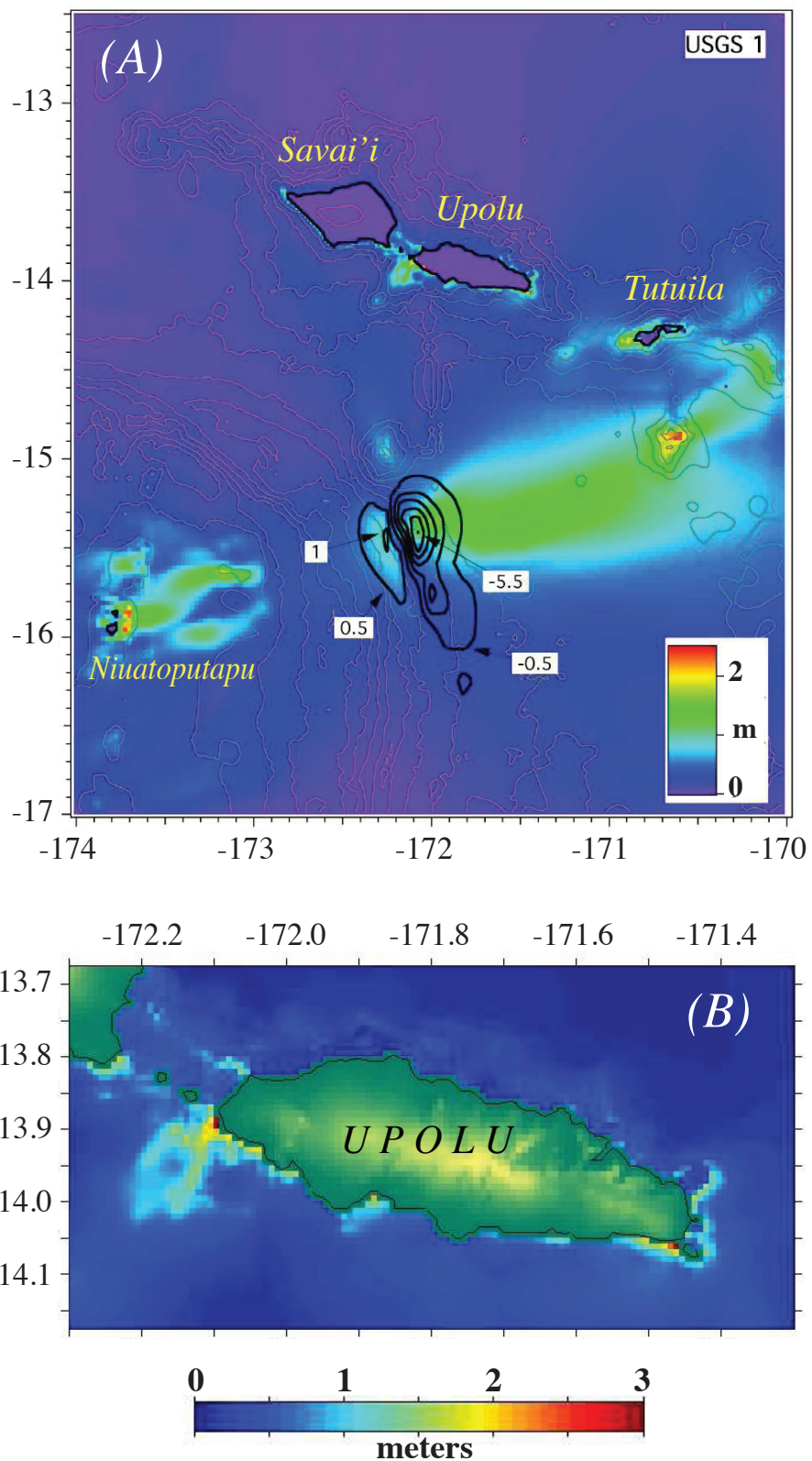
Thus this tsunami illustrates, once again, the value of education and preparedness of the populations at risk for the mitigation of natural hazards. ☒

ACKNOWLEDGMENTS

Field work was supported by the National Science Foundation under RAPID grant OCE-10-00694 to H.M.F. and C.E.S., and by a grant to E.A.O. from the Vice-President for Research, Northwestern University. Discussions with Steve Kirby on outer rise events are acknowledged. We are grateful to Catherine Chagué-Goff for sharing with us the lone eyewitness report of the 1917 event in Upolu. E. A. O. thanks Bernard Dost for hospitality at the seismological archives of the Royal Netherlands Meteorological Institute in De Bilt. Maps were drawn using the GMT software (Wessel and Smith 1991). C.E.S. thanks the Pacific Earthquake Engineering Research Institute (PEER) for partial support.

REFERENCES

- Briggs, M. J., C. E. Synolakis, G. S. Harkins, and D. R. Green (1995). Laboratory experiments of tsunami runup on a circular island. *Pure and Applied Geophysics* **144**, 569–594.
- Govers, R., and M. J. R. Wortel (2005). Lithosphere tearing at STEP faults: Response to edges of subduction zones. *Earth and Planetary Science Letters* **236**, 505–523.
- Gutenberg, B., and C. F. Richter (1954). *Seismicity of the Earth and Associated Phenomena*. Princeton, NJ: Princeton Univ. Press, 310 pp.
- Hart, S. R., H. Staudigel, A. A. P. Koppers, J. Blusztajn, E. T. Baker, R. Workman, M. Jackson, E. Hauri, M. Kurz, K. Sims, D. Fornari, A. Saal, and S. Lyons (2000). Vailulu'u undersea volcano: The new Samoa. *Geochemistry, Geophysics, Geosystems* **1**, GC000108.



▲ **Figure 8.** A) Map of the regional results of the simulation using Model USGS-1. The deep-water maximum amplitude of the tsunami is color-coded according to the vertical palette. The thick lines map the static field of displacement of the seismic source, with selected contours labeled (in meters). Note the focusing of the wave toward Niuatoputapu, and the general agreement of the predicted wave heights with our field surveys. B) Close-up of the simulated wavefield around Upolu. Note the predicted high amplitudes at both its southeastern tip (observed) and southwestern one (not observed).

- Hirshorn, B. F., N. Becker, and S. Weinstein (2009). The Pacific Tsunami Warning Center response to the $M_w = 8.1$ Samoan earthquake of September 29, 2009. *Eos, Transactions, American Geophysical Union* **90** (53), U13E-2083 (abstract).
- Imamura, F., E. Gica, T. Takahashi, and N. Shuto (1995). Numerical simulation of the 1992 Flores tsunami: Interpretation of tsunami phenomena in northeastern Flores Island and damage at Babi Island. *Pure and Applied Geophysics* **144**, 555–568.
- Jaffe, B. E., B. M. Richmond, G. R. Gelfenbaum, S. Watt, A. A. Apotos, M. L. Buckley, W. C. Dudley, and B. Peck (2009). Field observations of the 29 September tsunami in American Samoa: Spatial variability and indications of strong return flow. *Eos, Transactions, American Geophysical Union* **90** (52), U21E-2178 (abstract).
- Ji, C., D. J. Wald, and D. V. Helmlinger (2002). Source description of the 1999 Hector Mine earthquake, Part I: Wavelet domain inversion theory and resolution analysis. *Bulletin of the Seismological Society of America* **92**, 1,192–1,206.
- Kirby, S. H., R. Hino, N. Umino, S. Gamage, A. Hasegawa, E. R. Engdahl, and E. Bergman (2008). The 75th anniversary of the great Sanriku-oki, Japan earthquake of March 2nd, 1933: New observations and new insights into the largest recorded outer-rise earthquake. *Eos, Transactions, American Geophysical Union* **89** (53), S14A-05 (abstract).
- Koppers, A. A. P., J. A. Russell, M. G. Jackson, J. Konter, H. Staudigel, and S. R. Hart (2008). Samoa reinstated as a primary hotspot trail. *Geology* **36**, 435–438.
- Koshimura, S., Y. Nishimura, Y. Nakamura, Y. Namegaya, G. J. Fryer, A. Akapo, L. S. Kong, and D. Vargo (2009). Field survey of the 2009 tsunami in American Samoa. *Eos, Transactions, American Geophysical Union* **90** (52), U23F-07 (abstract).
- Lamarche, G., B. Pelletier, and J. Goff (2010). Impact of the 29 September 2009 South Pacific tsunami on Wallis and Futuna. *Marine Geology* **271**, 297–302.
- Lay, T., C. J. Ammon, and H. Kanamori (2009). Great Samoa earthquake ($M_w = 8.2$) of 29 September 2009. *Eos, Transactions, American Geophysical Union* **90** (53), U21D-05 (abstract).
- Li, X., G. Shao, and C. Ji (2009). Rupture process of $M_w = 8.1$ Samoa earthquake constrained by joint inverting teleseismic body, surface waves and local strong motion. *Eos, Transactions, American Geophysical Union* **90** (53), U21D-03 (abstract).
- Natland, J. H. (1980). The progression of volcanism in the Samoan linear volcanic chain. *American Journal of Science* **280-A**, 709–735.
- Newman, A. V., and E. A. Okal (1998). Teleseismic estimates of radiated seismic energy: The E/M_0 discriminant for tsunami earthquakes. *Journal of Geophysical Research* **103**, 26,885–26,898.
- Okada, Y. (1985). Surface deformation due to shear and tensile faults in a half-space. *Bulletin of the Seismological Society of America* **75**, 1,135–1,154.
- Okal, E. A. (1992). Use of the mantle magnitude M_m for the reassessment of the seismic moment of historical earthquakes. I: Shallow events. *Pure and Applied Geophysics* **139**, 17–57.
- Okal, E. A., J. C. Borrero, and C. E. Synolakis (2004). The earthquake and tsunami of 17 November 1865: Evidence for far-field tsunami hazard from Tonga. *Geophysical Journal International* **157**, 164–174.
- Okal, E. A., and C. J. Hartnady (2009). The South Sandwich Islands earthquake of 27 June 1929: Seismological study and inference on tsunami risk for the South Atlantic. *South African Journal of Geology* **112**, 359–370.
- Regelous, M., S. Turner, T. J. Falloon, P. Taylor, J. Gamble, and T. Green (2008). Mantle dynamics and mantle melting beneath Niuafo'ou Island and the northern Lau back-arc basin. *Contributions in Mineralogy and Petrology* **156**, 103–118.
- Solov'ev, S. L., and C. N. Go (1984). Catalogue of tsunamis on the eastern shore of the Pacific Ocean. *Can. Transl. Fish. Aquat. Sci.* **5078**, 293 pp.
- Solov'ev, S. L., C. N. Go, and K. S. Kim (1986) *Katalog tsunami v tikhom okeane, 1969–1982 gg.* Moscow: Akad. Nauk SSSR, 164 pp. (in Russian).
- Synolakis, C. E., and E. A. Okal (2005). 1992–2002: Perspective on a decade of post-tsunami surveys, in *Tsunamis: Case Studies and Recent Developments*, ed. K. Satake. *Advances in Natural and Technological Hazards* (Dordrecht: Kluwer) **23**, 1–30.
- Titov, V. V., F. I. González, E. N. Bernard, M. C. Eble, H. O. Mofjeld, J. C. Newman, and A. J. Venturato (2005). Real-time tsunami forecasting: Challenges and solutions. *Natural Hazards* **35**, 35–41.
- Titov, V. V., and C. E. Synolakis (1998). Numerical modeling of tidal wave runup. *Journal of Waterways, Port and Coastal Engineering* **B124**, 157–171.
- Turner, S., and C. Hawkesworth (1997). Constraints on flux rates and mantle dynamics beneath island arcs from Tonga-Kermadec lava geochemistry. *Nature* **389**, 568–573.
- Wendt, J. I., M. Regelous, K. D. Collerson, and A. Ewart (1997). Evidence for a contribution from two mantle plumes to island-arc lavas from northern Tonga. *Geology* **25**, 611–614.
- Wessel, P., and W. H. F. Smith (1991). Free software helps map and display data. *Eos, Transactions, American Geophysical Union* **72**, 441, 445–446.
- Workman, R. K., S. R. Hart, M. Jackson, M. Regelous, K. A. Farley, J. Blusztajn, M. Kurz, and H. Staudigel (2004). Recycled metasomatized lithosphere as the origin of the Enriched Mantle II (EM2) end-member: Evidence from the Samoan volcanic chain. *Geochemistry, Geophysics, Geosystems* **5**, Q04008.
- Wyssession, M. E., E. A. Okal, and K. L. Miller (1991). Intraplate seismicity of the Pacific Basin, 1913–1988. *Pure and Applied Geophysics* **135**, 261–359.
- Yeh, H., P.-L. Liu, M. Briggs, and C. E. Synolakis (1994). Propagation and amplification of tsunamis at coastal boundaries. *Nature* **372**, 353–355.

*Department of Earth and Planetary Sciences
Northwestern University
Evanston, Illinois 60208 U.S.A.
emile@earth.northwestern.edu
(E. A. O.)*